Supporting Information

Composition-tuned $MAPbBr_3$ nanoparticles with addition of Cs^+ cation for improved photoluminescence.

Sai S.H. Dintakurti,*[abc] Parth Vashishtha,[b] David Giovanni,[d] Yanan Fang,[b] Norton Foo, [b] Zexiang Shen,[ade] Claude Guet, [a] Tze Chien Sum,[d] Tim White,*[b]

[a] ERI@N, Interdisciplinary Graduate School, Nanyang Technological University, Singapore 639798
[b] School of Materials Science and Engineering, Nanyang Technological University, Singapore 639798
[c] Department of Physics, University of Warwick, Coventry, West Midlands, United Kingdom, CV4 7AL
[d] School of Physical and Mathematical Sciences, Nanyang Technological University, Singapore 639798
[e] Centre for Disruptive Photonic Technologies, and CNRS International NTU Thales Research Alliance, Nanyang Technological University, Singapore 639798

Corresponding email: sriharsh001@e.ntu.edu.sg; tjwhite@ntu.edu.sg

Experimental details

Chemicals and Reagents

Cesium Bromide (99.999% trace metal basis, Aldrich), Lead Bromide (99.999% trace metal basis, Aldrich), Methylammonium Bromide (99.99%, Greatcell Solar), Dibenzo-21-crown-7 ether (Aldrich, 97%), N,N - Dimethylformamide (anhyd. 99.8% Aldrich), Toluene (anhyd. 99.8% Aldrich), Octylamine (99%, Aldrich), Oleic acid (90%, Aldrich), Methyl acetate (99%, Aldrich) and Hexane (anhyd. 95% Aldrich).

Synthesis

The synthesis of $MA_xCs_{1-x}PbBr_3$ nanoparticles was undertaken using the previously reported ligand assisted reprecipitation (LARP) method.[1-3] To overcome poor solubility of CsBr, a cesium selective crown ether was added to dissolve the cesium halide salt. A 0.2M perovskite solution was prepared from stoichiometric mixture of CsBr, MABr and $PbBr_2$ along with equimolar (in comparison to CsBr) dibenzo-21-crown-7 ether were dissolved in 2 ml DMF

inside a nitrogen-filled glove box (see Table S5 for details). 150 µL of this precursor solution was drop-casted in a solution containing 5 mL of toluene with 21 µL of octylamine and 471 µL of oleic acid under continuous stirring. After resting for ~5 min, a bright green colour solution developed which was centrifuged at 10,000 rpm for 10 min, and the precipitate was washed with 80 µL methylacetate and re-dispersed in 300 uL of anhydrous hexane. Thus synthesized nanoparticles were purified by centrifuging at 1000 rpm for 5 min, discarding the precipitate to obtain ink suitable for LED fabrication.

LED fabrication

Patterned ITO glass substrates (sheet resistance ~8 Ωcm-1) were cleaned using consecutive 20 min sonication cycles in Hellmanex (10 % solution in deionized water), deionized water, acetone and isopropanol, followed by UV-ozone treatment for 15 min. A filtered solution of PEDOT:PSS (Clevios Al4083) was spin coated on a cleaned ITO substrate at 4000 rpm for 60 s followed by annealing at 130 °C for 20 min. PEDOT:PSS coated substrates were then transferred to an argon-filled glove box for further processing. Poly-TPD (2.5 mg ml^{-1}) was spin coated at 4000 rpm for 60 s followed by annealing at 140 °C for 30 min. Perovskite nanoparticles (in hexane) were spin coated at 2000 rpm (acceleration = 500 rpm s^{-1}) for 60 s. A 20 nm layer of POT2T was thermally evaporated under 10^{-6} Torr vacuum. 0.8 nm LiF and 80 nm Al electrode were finally evaporated through a shadow mask. All LEDs were encapsulated using UV-curable epoxy resin before removing from the glove box for electrical characterisation.

LED Measurements

LED Measurement: A Keithley 2612B measurement unit was used to obtain the current-voltage characteristics of the LED devices using a scan rate of 1 V s^{-1}, step size of 0.1 V and a step interval of 0.1 s. The emitted light was collected by an Ocean Optics FOIS-1 integrating sphere coupled to a calibrated spectrophotometer (Ocean Optics QEPro) through an optical fibre. An Ocean Optics HL-3 Plus vis-NIR light source was used for calibration of absolute irradiance measurement of the spectrometer. LEDs were placed on the port of the integrating sphere and only forward emission was captured while the edge emission contribution was lost outside the integrating sphere. This method has also been widely used to measure the external quantum efficiency of LEDs.[1, 2, 4-6]

Powder X-ray Diffraction

A Panalytical X-ray diffractometer equipped with a 1.8kW Cu Kα X-ray tube and operating in a Bragg Brentano geometry was used to collect the diffractograms. The X-ray source was operated at 40 kV and 30 mA along with a 1D detector having an active length of 2.122° to collect data in the 2θ range of 5 - 90°. The nanoparticles suspensions were drop casted on zero background Si single crystal sample holder, which was rotated at 20 rpm during the measurement. The obtained data was fitted using a Rietveld refinement using TOPAS v6 software. A cubic model where the disordered methylammonium ion was approximated to a sphere was used to fit the data.

X-ray Photoelectron Spectroscopy

X-ray photoelectron spectroscopy (XPS) analysis was performed using a Kratos AXIS Supra spectrometer with a monochromatic Al K-alpha source (15 mA, 15 kV). An area scan was used for elemental analysis. Measurements were performed on drop casted samples on a conductive glass substrate. The spectra were calibrated by setting the C 1s peak to 284.8 eV. The nanoparticles being stabilized by the oleic acid and octylamine ligands give rise to an easily detectable C 1s signal. The background correction, calibration and quantification were done using ESCApe software. Cs 4d, Pb 4f and Br 3d peaks have been integrated, corrected for sensitivity and then used to calculate the atomic concentrations reported in Table S4.

Transmission Electron Microscopy

High-resolution transmission electron microscopy (HR-TEM) was carried out using a JEOL 2010 UHR TEM with a field-emission gun operating at 200 kV of accelerating voltage and 108 μA of beam current. Samples were prepared by diluting purified nanoparticles in anhydrous hexane. The sample was then drop casted on a Cu-200 mesh on forvar grid. Observation times were limited to a few minutes due to electron amorphization, especially when a more converged beam was used for imaging. Approximately 150 particles were measured for each sample to estimate the average size of nanoparticles using ImageJ software.[7]

UV-Vis Spectroscopy

The absorption spectra were collected using a Cary 5000 UV–vis–NIR spectrophotometer. Each sample was prepared by diluting the purified nanoparticles in hexane in a 1 cm path length quartz cuvettes. A baseline was corrected using only hexane solvent before measurements.

Photoluminescence Measurements

All PL measurements were performed using a Cary Eclipse spectrophotometer. The same solution of nanoparticles as UV-Vis measurements were used to collect the PL measurements at excitation wavelength of 400 nm with 1 nm slit-width.

Photoluminescence quantum yield (PLQY) dependencies on the excitation fluence were measured with a Thorlabs IS20 integrating sphere. Purified nanoparticle suspensions in a cuvette were placed inside the sphere and excited using a 200mW and 445 nm continuous-wave laser beam. An optical fibre was attached to the sphere to direct the light to an Ocean Optics spectrometer. The excitation beam intensity was attenuated by means of calibrated Thorlabs neutral interference filters. This method has been widely used for PLQY measurements.[4, 5]

The PL lifetime was measured by first collecting the PL using a lens pair, before directing the emission toward a Princeton Instrument SP2360i monochromator coupled with Optoscope streak camera. Nanoparticle solutions were photoexcited using a 400 nm ~50 fs pulsed laser, with 1 kHz repetition rate.

Table S1. Refined XRD parameters obtained from Rietveld refinement of the powder diffraction data.

Sample	**R_b**	***a*** **(Å)**	**Unit cell voume ($Å^3$)**
Cs100	1.4	5.864(4)	201.7
Cs87	1.5	5.875(4)	202.8
Cs75	3.5	5.879(3)	203.2
Cs63	3.2	5.879(3)	203.2
Cs50	9.2	5.886(2)	203.9
Cs37	2.5	5.891(7)	204.5
Cs25	3.7	5.908(0)	206.2
Cs13	5.3	5.917(4)	207.2
Cs0	6.08	5.929(3)	208.4

Table S2. Biexponential fitting parameters extracted from TRPL spectra to obtain charge carrier lifetime. t1 and t2 represent the nonradiative and radiative lifetimes respectively. The ratio between them is given as A1/A2.

Equation	**y = A1*exp(-x/t1) + A2*exp(-x/t2) + y0**						
Sample	**a1**	**t1**	**a2**	**t2**	**A1 (Nonradiative)**	**A2 (radiative)**	**t_{ave}**
Cs0	0.22	7.94	0.81	30.42	0.22	0.78	25.59
Cs13	0.24	3.65	0.76	22.52	0.25	0.75	17.88
Cs25	0.47	4.55	0.54	25.37	0.47	0.53	15.58
Cs37	0.39	3.67	0.56	24.31	0.41	0.59	15.76
Cs50	0.46	3.21	0.54	26.40	0.46	0.54	15.65

Cs63	0.62	3.04	0.38	20.92	0.62	0.37	9.74
Cs75	0.59	2.72	0.35	22.10	0.63	0.37	9.85
Cs87	0.43	2.64	0.54	14.80	0.45	0.56	9.39
Cs100	0.57	2.76	0.48	21.18	0.55	0.45	11.07

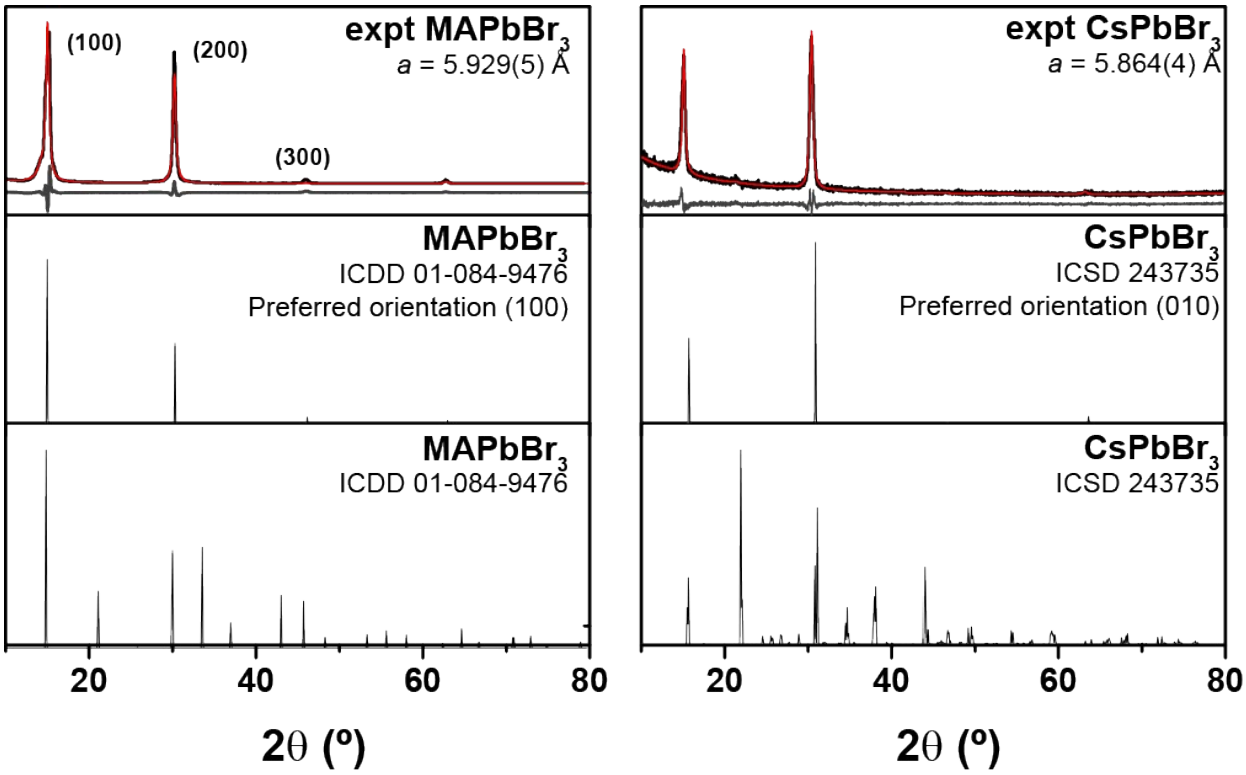

Figure S1. *Comparison of standard PXRD, with preferred orientation effects and the experimental data for $MAPbBr_3$ and $CsPbBr_3$ nanoparticles.*

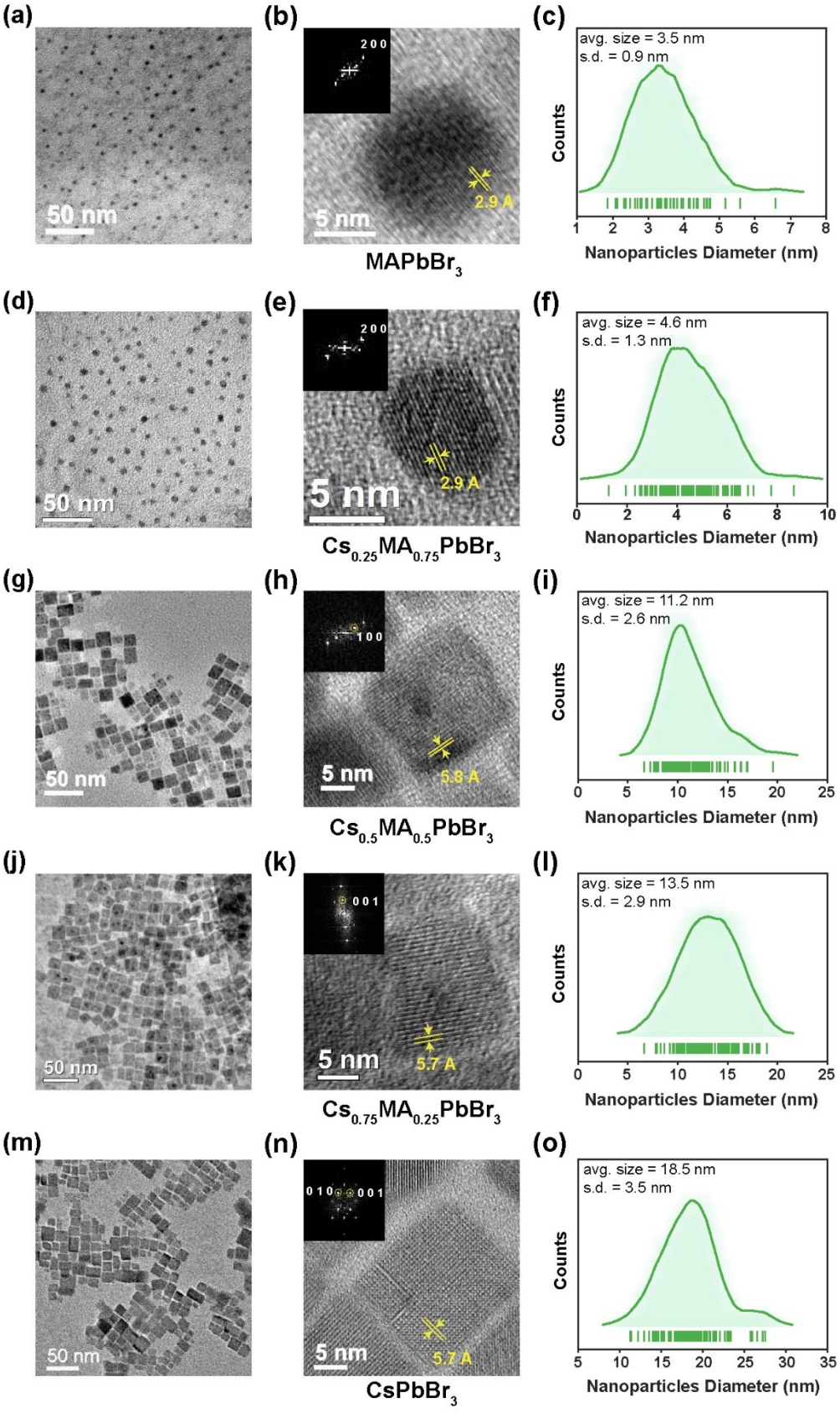

Figure S2. *(a-o)High resolution TEM images and average shifted histograms estimating the particle size distribution in Cs0, Cs25,Cs50,Cs75 and Cs100 samples.*

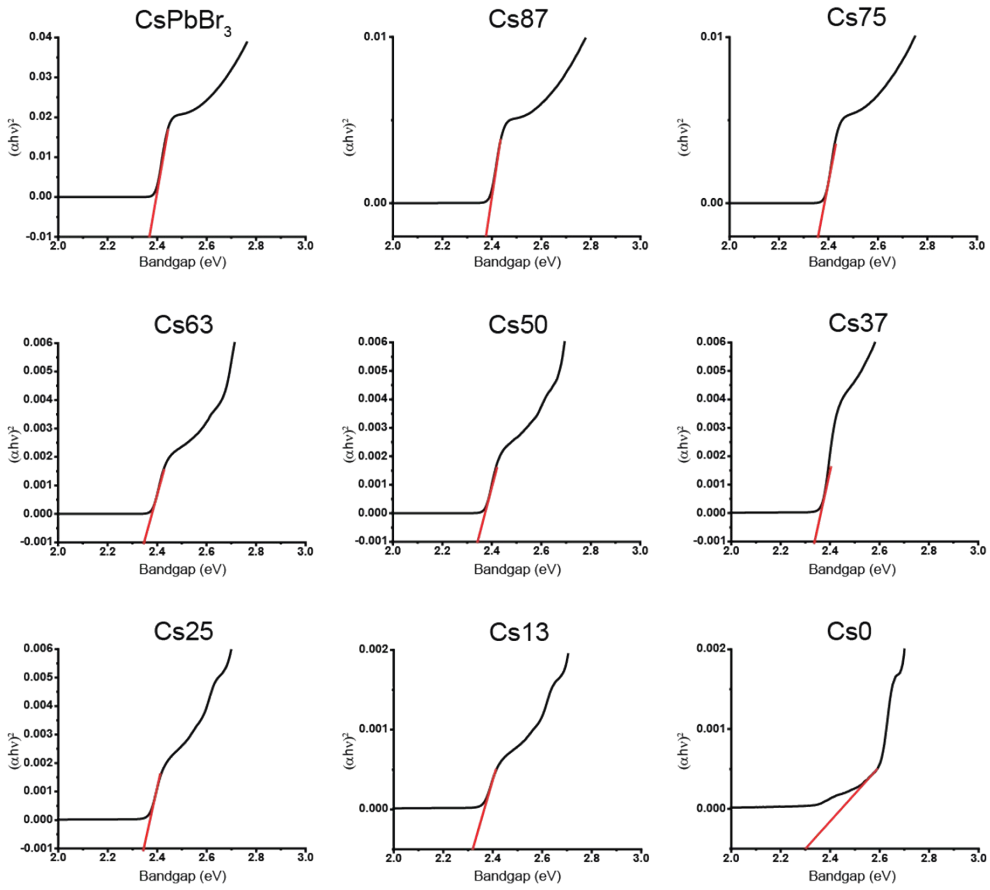

Figure S3. *Tauc plots of UV-vis absorption spectra used for estimating bandgap in Table 1.*

Table S3. Device matrices for as fabricated LEDs

Device Name	**EL Peak Position (nm)**	**Current Efficiency (cd A^{-1})**	**Power Efficiency (lm W^{-1})**	**EQE (%)**
Cs100	518	0.64	0.41	0.20
Cs13	522	2.83	2.34	0.83

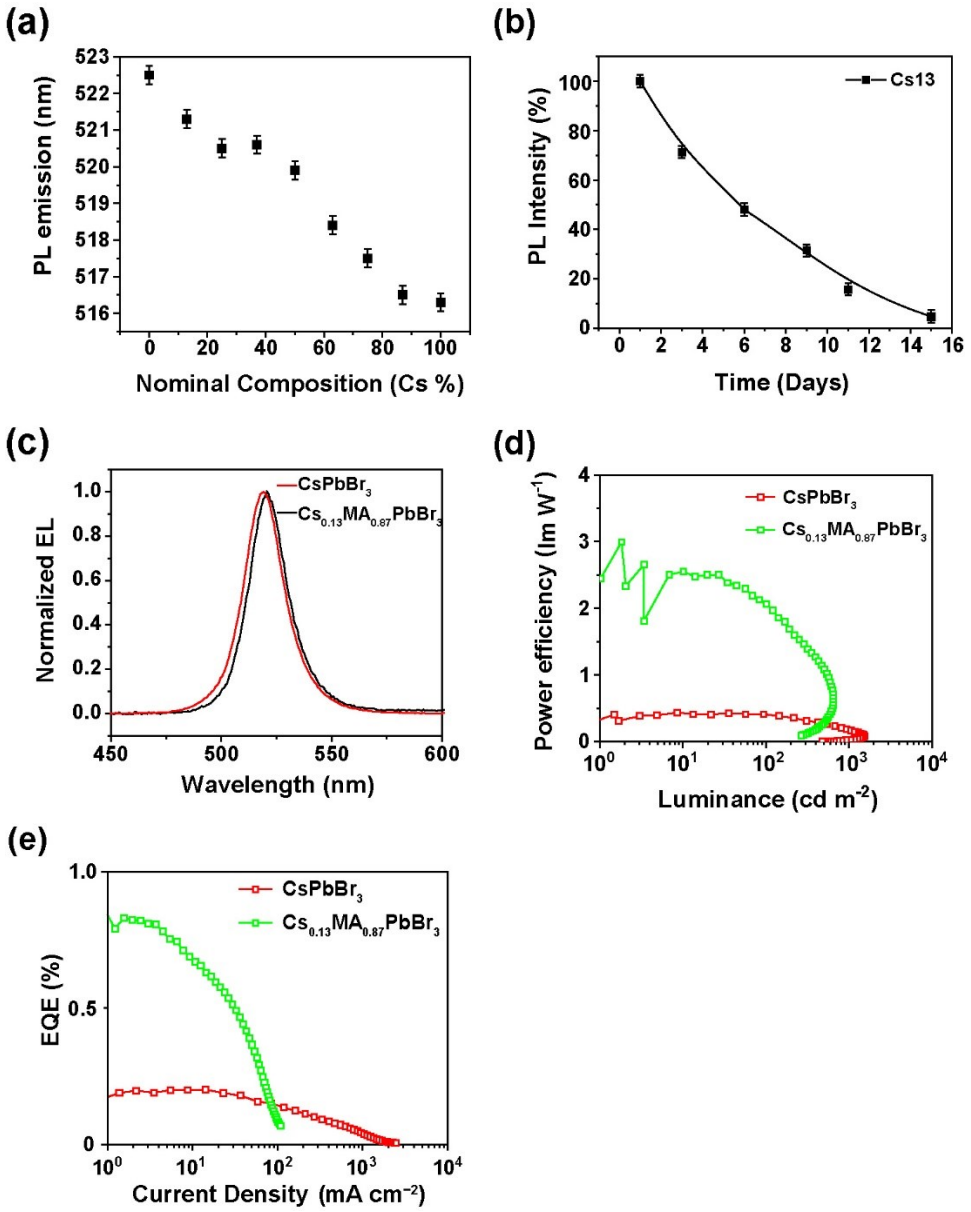

Figure S4. *(a) Plot of PL emission vs composition showing a slight deviation around 50% Cs composition due to a higher Cs content as evident from XRD and XPS data. (b) PL stability data of Cs13 sample. (c) EL spectra, (d) Power efficiency vs luminance, and (e) current efficiency vs current density diagram of as fabricated LEDs.*

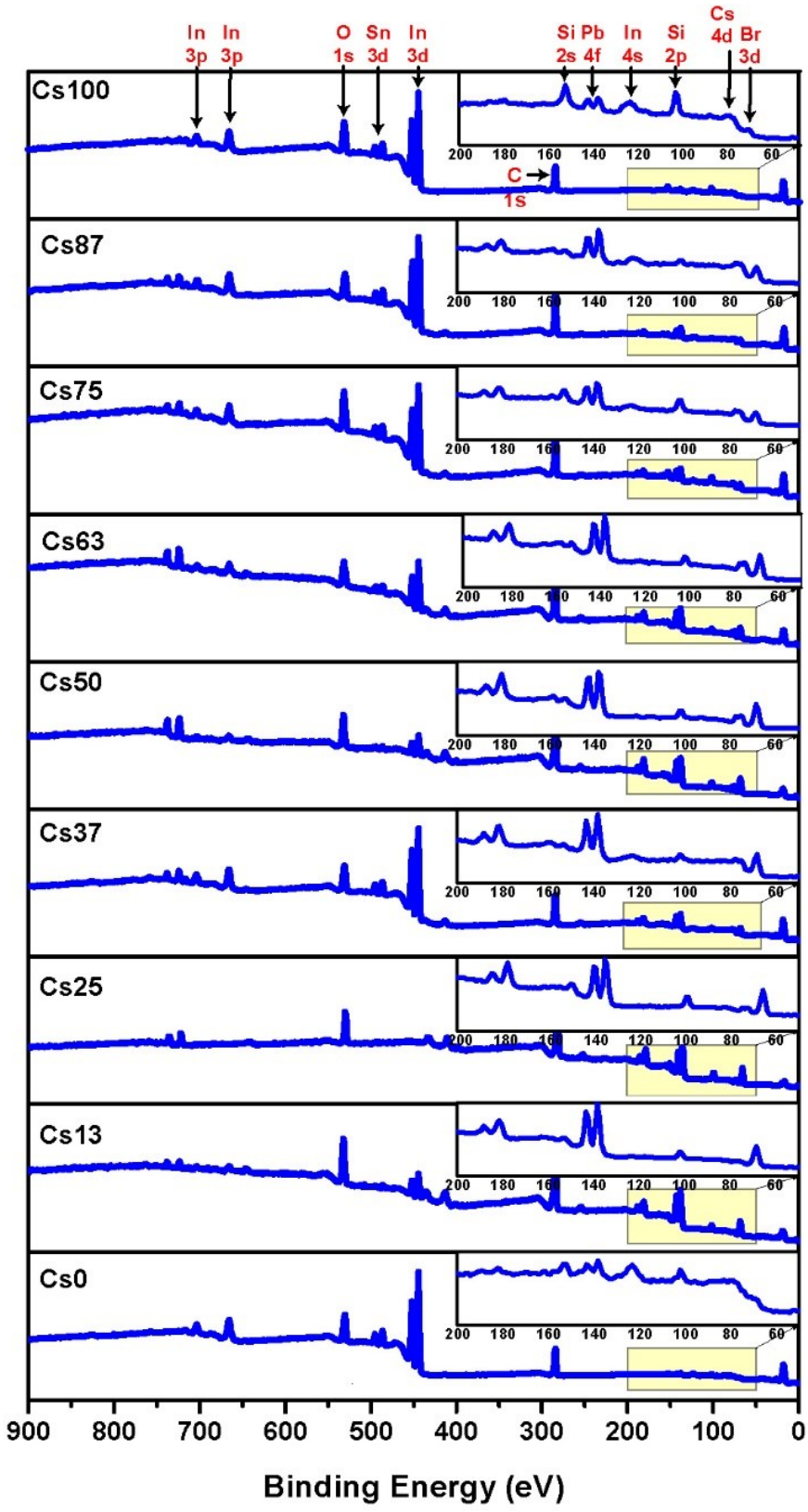

Figure S3. *X-ray photoelectron spectroscopy (XPS) survey scan data of the prepared nanoparticle samples of the solid solution series* $MA_xCs_{1-x}PbBr_3$*. The nanoparticle samples have been dropcasted onto ITO coated glass resulting in In, Sn, Al, Si and O peaks.*

Table S4. Elemental composition obtained from XPS analysis.

Sample	Cs at. % (± 2%)	Pb at.% (± 1%)	Br at % (± 3%)	Cs content as a fraction of Pb
Cs100	19.8	20.5	59.7	0.97
Cs87	18.1	20.3	61.6	0.89
Cs75	14.7	19.5	65.8	0.75
Cs63	13.6	18.6	67.8	0.73
Cs50	12.6	18.1	69.3	0.69
Cs37	11.0	18.2	70.8	0.58
Cs25	7.4	21.8	70.9	0.34
Cs13	3.2	24.8	72.0	0.13
Cs0	0.0	26.9	73.1	0.0

Table S5. Materials and quantities used for preparation of perovskite precursor solution in DMF.

Composition	CsBr (mg)	Dibenzo 21-crown-7 ether (mg)	MABr (mg)	$PbBr_2$ (mg)	$PbBr_2$ (mMol)	DMF (ml)
Cs0	0.00	0.00	44.79	146.80	0.40	2.00
Cs13	11.07	21.03	38.97	146.80	0.40	2.00
Cs25	21.28	40.45	33.59	146.80	0.40	2.00
Cs37	31.49	59.87	28.22	146.80	0.40	2.00
Cs50	42.56	80.90	22.39	146.80	0.40	2.00
Cs63	53.63	101.93	16.57	146.80	0.40	2.00
Cs75	63.84	121.35	11.20	146.80	0.40	2.00
Cs87	74.05	140.77	5.82	146.80	0.40	2.00
Cs100	85.12	161.80	0.00	146.80	0.40	2.00

References

1. P. Vashishtha, S. A. Veldhuis, S. S. Dintakurti, N. L. Kelly, B. E. Griffith, A. A. Brown, M. S. Ansari, A. Bruno, N. Mathews and Y. Fang, *Journal of Materials Chemistry C*, 2020, **8**, 11805-11821.
2. S. A. Veldhuis, Y. F. Ng, R. Ahmad, A. Bruno, N. F. Jamaludin, B. Damodaran, N. Mathews and S. G. Mhaisalkar, *ACS Energy Letters*, 2018, **3**, 526-531.
3. P. Vashishtha, S. A. Veldhuis, S. S. H. Dintakurti, N. L. Kelly, B. E. Griffith, A. A. M. Brown, M. S. Ansari, A. Bruno, N. Mathews, Y. Fang, T. White, S. G. Mhaisalkar and J. V. Hanna, *Journal of Materials Chemistry C*, 2020, DOI: 10.1039/D0TC02038A.
4. A. A. M. Brown, T. J. N. Hooper, S. A. Veldhuis, X. Y. Chin, A. Bruno, P. Vashishtha, J. N. Tey, L. Jiang, B. Damodaran and S. H. Pu, *Nanoscale*, 2019.
5. X. Y. Chin, A. Perumal, A. Bruno, N. Yantara, S. A. Veldhuis, L. Martínez-Sarti, B. Chandran, V. Chirvony, A. S.-Z. Lo and J. So, *Energy & Environmental Science*, 2018, **11**, 1770-1778.
6. P. Vashishtha and J. E. Halpert, *Chemistry of Materials*, 2017, **29**, 5965-5973.
7. J. Schindelin, I. Arganda-Carreras, E. Frise, V. Kaynig, M. Longair, T. Pietzsch, S. Preibisch, C. Rueden, S. Saalfeld, B. Schmid, J.-Y. Tinevez, D. J. White, V. Hartenstein, K. Eliceiri, P. Tomancak and A. Cardona, *Nature Methods*, 2012, **9**, 676-682.